ISSN 0965-5425, Computational Mathematics and Mathematical Physics, 2015, Vol. 55, No. 9, pp. 1567–1578. © Pleiades Publishing, Ltd., 2015.
Original Russian Text © Yu.V. Vassilevski, V.Yu. Salamatova, S.S. Simakov, 2015, published in Zhurnal Vychislitel'noi Matematiki i Matematicheskoi Fiziki, 2015, Vol. 55, No. 9, pp. 1599–1610.

In blessed memory of A.P. Favorskii

On the Elasticity of Blood Vessels in One-Dimensional Problems of Hemodynamics

Yu. V. Vassilevski[a,b], V. Yu. Salamatova[a,b], and S. S. Simakov[a,b,c]

[a] *Moscow Institute of Physics and Technology, Institutskii per. 9, Dolgoprudnyi, Moscow oblast, 141700 Russia*
[b] *Institute of Numerical Mathematics, Russian Academy of Sciences, ul. Gubkina 8, Moscow, 119333 Russia*
[c] *Institute of Computer-Aided Design, Russian Academy of Sciences, Vtoraya Brestskaya ul. 19/18, Moscow, 123056 Russia*
e-mail: yuri.vasilevski@gmail.com, simakovss@ya.ru, salamatova@gmail.com

Received February 26, 2015

Abstract—One-dimensional models of hemodynamics proved to be effective in the analysis of blood flow in humans in the normal and pathological states. A key factor contributing to the successful simulation using one-dimensional models is the inclusion of elastic properties of blood vessel walls. This paper is devoted to the comparative analysis of various mathematical descriptions of elastic properties of vessel walls in modern one-dimensional models of hemodynamics.

DOI: 10.1134/S0965542515090134

Keywords: mathematical modeling, hemodynamics, blood vessel, constitutive equations.

1. INTRODUCTION

Approaches to modeling the blood flow using one-dimensional network models have been successfully developed in recent decades. This class of models proved to be effective in the investigation of the global blood flow in humans, of transport of various substances by blood, and of specific features of hemodynamics under pathological changes in the organism. One of the first network dynamic models was developed by the team of researchers under the guidance of Favorskii (see [1–5]). A number of mathematical problems concerning the statement and solution of the boundary value problem of the graph of vessels were solved. Physiological aspects related to the neuroregulation of vascular tone were examined. Models of substance transport and blood flow under g-loads were constructed, and several versions of state equations describing the elasticity of vessel walls were investigated.

Modeling the elasticity of blood vessel walls is a key issue in one-dimensional modeling of hemodynamics. Presently, several mathematical formulations are available. Despite their differences, they are successfully used not only for qualitative but also for quantitative personalized hemodynamic calculations.

This paper is devoted to the comparative analysis of various mathematical descriptions of elastic properties of vessel walls in modern one-dimensional models of hemodynamics. In Section 2, a brief description of the anatomical structure of vessels of various types is given. Section 3 is devoted to the discussion of various phenomenological models of elasticity of vessel walls. In Section 4, a general description of the most popular mathematical formulation of elasticity properties of large arteries and veins used in one-dimensional models of hemodynamics is given. The data of medical investigations of the human common carotid artery, human common femoral artery, and canine common femoral vein are used to adjust each model. We compare the numerical results of the propagation of a single impulse in a single vessel whose elastic properties are simulated using each model. The main differences in the systolic pressure, pulse wave propagation rate, and formation of shock waves are analyzed.

2. ANATOMICAL STRUCTURE OF VESSEL WALLS

Blood vessels are elastic tubular formations that transport blood throughout the entire organism. Depending on the direction of blood flow relative to the heart, the blood vessels are classified into veins and arteries. The size of vessels and their morphology depend on their place in the vascular network, age, systemic diseases, etc.

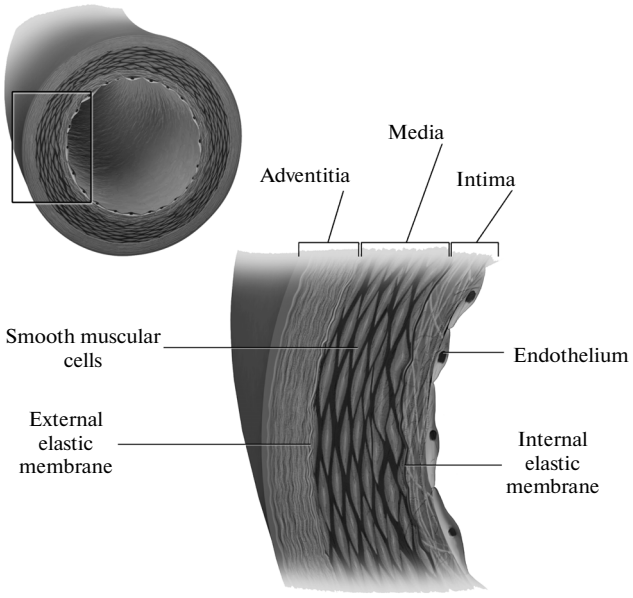

Fig. 1. Typical structure of the blood vessel wall (see [6]).

The wall of a blood vessel (except for capillaries) can be divided into three layers—internal layer (tunica intima), middle layer (tunica media), and external layer (tunica adventitia), see Fig. 1.

The basic structure elements of blood vessels are as follows: endothelial cells, collagen fibers, elastin fibers, smooth muscular cells, and the main substance that joins all the elements. Depending on the morphological composition of a vessel wall, arteries can be classified into elastic and muscular ones (see [7]). Elastic arteries have a relatively large diameter and are closer to the heart (e.g., aorta or carotid artery); their media contains a lot of elastic membranes. The number of elastic membranes decreases with decreasing vessel size (i.e., when the vessels become father from the heart). Muscular arteries have almost no elastic membranes. Muscular arteries are at the periphery (e.g., the femoral artery, abdominal artery, or cerebral arteries). The middle layer of muscular arteries mainly consists of smooth muscular cells. There are arteries with a combined internal structure of the walls (elastic muscular arteries).

In contrast to arteries, veins are classified by their internal diameter. The walls and the middle layer of veins are much thinner than those of arteries. However, veins have a thicker external layer (adventitia). Large veins can have valves to pass the blood only in one direction.

Consider specific features of the structure of each of the three layers depending on the vessel type.

Intima—the internal layer of all blood vessels—consists of (1) a layer of endothelial cells that line the vessel wall, (2) a thin basal membrane, and (3) a subendothelial layer consisting of collagen fibers, elastic fibrils, smooth muscular cells, and some amount of fibroblast. The subendothelial layer is present only in large human elastic arteries. In all other blood vessels, the intima consists of a layer of endothelial cells and a basal membrane.

Media—the internal layer of blood vessels—consists of smooth muscular cells, a certain number of elastic membranes, and elastin and collagen fibers. There may be no smooth muscular cells in large veins, but they are prevalent in the media of the majority of vessels. This layer is thicker in arteries than in veins. In arteries, fenestrated elastic membranes (about several tens) divide the media into concentric layers. These layers form a complex three-dimensional network of smooth muscular cells, elastin, and collagen. The number of elastic membranes decreases with decreasing size of the arteries. There are practically no elastic membranes in muscular arteries. In muscular arteries, one can clearly discern an internal elastic membrane and an external elastic membrane. For elastic arteries, they are indistinguishable from the internal elastic membranes. The media of veins typically consists of two or three layers of smooth muscular cells and bundles of collagen and elastin fibers.

Adventitia—the external layer of the blood vessel wall—consists of fibroblasts, fibrocytes, and bundles of collagen fibers. The external layer of all arteries and the majority of veins (except for large ones) do not contain smooth muscular cells. In almost all the vessels, collagen fibers are the prevailing structure component in the adventitia. The thickness of the external layer depends on the type and location of the vessel.

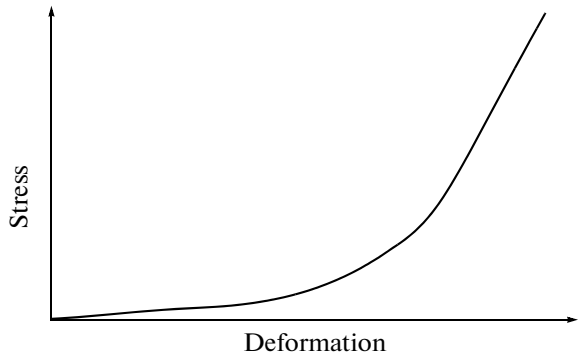

Fig. 2. Schematic curve of the blood vessel wall deformation.

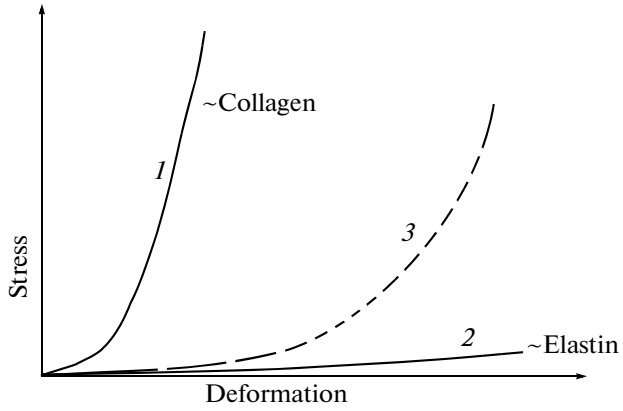

Fig. 3. Schematic curves of the artery wall deformation: *1* for removal of elastin from the wall; *2* for removal of collagen from the wall; *3* in the presence all the structural components.

For example, the cerebral vessels have no adventitia, while this layer is thicker in muscular arteries than in elastic arteries. In veins of medium and large size, the external layer is the thickest one.

A detailed description of the structure of blood vessels can be found in [7].

3. MODERN MODELS OF VESSEL WALL ELASTICITY

It is seen from the description above that the walls of blood vessels consist of a complex composite material, which can be represented by an isotropic matrix reinforced by differently oriented groups of fibers. The material of vessel walls is nonlinear, anisotropic, and weakly compressible (see [8, 9]). This material can be described by the finite deformation model, which assumes a geometric nonlinearity of vessel wall deformation models. Figure 2 shows a typical deformation curve of a blood vessel wall.

The mechanical properties of blood vessels are classified into passive (which do not take into account smooth muscular contractions) and passive–active (which take such contractions into account). In the majority of experimental studies only passive mechanical properties are considered. In this case, it is assumed that the elastic properties of blood vessels depend on the spatial arrangement of the main elastic fibers (elastinic and collagen ones) and their functional features are related to vessel deformations. The elastin fibers are fairly soft (the modulus of elasticity is about 10^5 Pa), while this modulus for the collagen fibers, which play the major role in maintaining the structural integrity of vessel walls, is about 10^8 Pa. The contribution of collagen and elastin to the rigidity of the iliac artery was studied in [10]. It was shown that in the case of low pressure, the major role is played by elastinic fibers. As the pressure increases, the contribution of collagen fibers increases. The load is distributed between the elastin and collagen. As the load increases further, the collagen becomes the major load-carrying element. The progressive involvement of different fibers is illustrated in Fig. 3. At the physiological level of pressure in arteries, both the elastin and

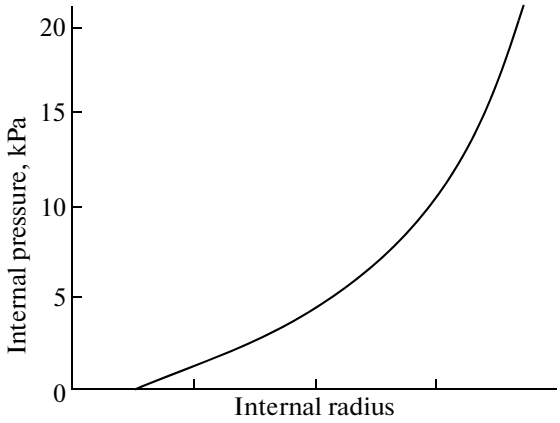

Fig. 4. Schematic curve of the dependence of pressure on the internal diameter of a circular cylinder based on the results obtained in [18].

collagen are involved in the load distribution, which corresponds to increasing slope of the tangent to the plot of the deformation curve in Fig. 3.

The account for the nonlinear mechanical properties of blood vessels is an important condition for their modeling. The nonlinearity must be included in the constitutive equations. The issue of constitutive equations for blood vessel walls has been under intensive development in recent decades. The state of the art and the history of this problem are described in [8, 11–13]. Recently, works devoted to the construction of constitutive equations based on the internal microstructure of vessel walls have appeared (see [14–16]).

The constitutive equations are determined by the form of the elastic deformation energy (elastic potential). There are a lot of papers devoted to this issue in the case of arteries. Various forms of deformation energy based on experimental data are considered. Due to significant differences in the structure of vessels depending on their location in the vascular system, none of the proposed versions is universal for all types of arteries. The most interesting among the proposed form of the elastic deformation energy are the versions proposed in [17–19].

In [18], the dependence of the stress-strain state of a thick wall cylinder occurring under the action of tensile and torsional loads on the form of the elastic deformation energy was analyzed. The elastic potentials that are widely used for modeling deformations of artery walls were selected from the family of elastic potentials. Almost all of them have a term that exponentially depends on the components of the right Cauchy–Green strain tensor. Limitations of the proposed models are discussed in [18]. These limitations are due to the representation of the vessel wall as an isotropic material and the limited application of the proposed models to a small class of loads.

As a result of solving the problem of deformation of a thick wall cylinder the action of tensile loads and a torque for different types of constitutive equations, dependences of the internal pressure on the internal radius were obtained in [18]. All the plots are similar (see Fig. 4)—the tangent slope increases with increasing vessel radius.

The constitutive equations proposed in [9] take into account the anisotropy of the wall material, and they are widely used in applications. The deformation energy function is represented in the form

$$\Psi = \Psi_{\text{iso}} + \Psi_{\text{aniso}}, \tag{3.1}$$

where the first term Ψ_{iso} describes the isotropic contribution of the wall material without taking collagen into account; this term is determined by the isotropic neo-Hookean model

$$\Psi_{\text{iso}} = \mu(I_1 - 3), \tag{3.2}$$

The second term Ψ_{aniso} in (3.1) describes the involvement of two families of collagen fibers, which increases the rigidity of the wall material. Ψ_{aniso} is represented by the anisotropic function

$$\Psi_{\text{aniso}} = \frac{k_1}{2k_2}(\exp\{k_2(I_4 - 1)^2\} - 1) + \frac{k_3}{2k_4}(\exp\{k_4(I_6 - 1)^2\} - 1). \tag{3.3}$$

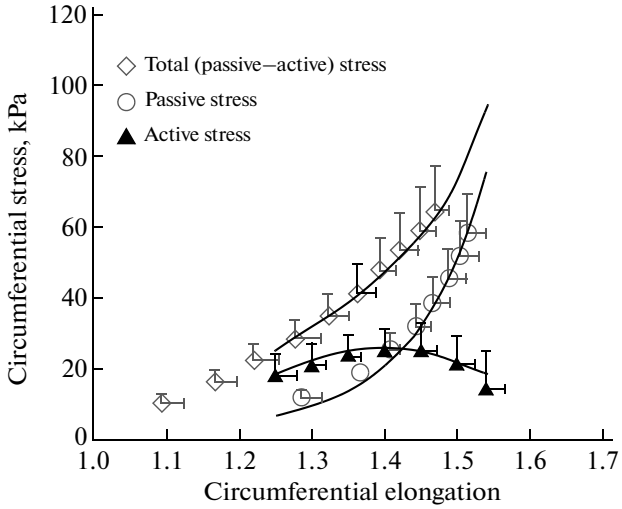

Fig. 5. Experimental dependence of the circumferential stresses on the circumferential elongation depending on contractions of smooth muscular cells for the media of the pig coronary artery [14].

In (3.2) and (3.3), μ, k_1, k_2, k_3, and k_4 are constants depending on the material; I_1 is the first invariant of the Cauchy–Green strain tensor; and I_4 and I_6 are the invariants characterizing the degree of stretching of the fibers of the corresponding family.

A model that takes into account different orientations of the collagen fibers in the vessel wall was proposed in [19]. The mechanical properties of each individual layer were studied in [20]. The resulting constitutive equations for each layer have form (3.2) and (3.3).

The number of studies devoted to veins is not large. In [21], the passive mechanical properties of the cava in rats were investigated, and the phenomenological model

$$\Psi = \frac{c_{\text{el}}}{\lambda_{\text{el, max}} - \lambda_z - c_{\text{inel}}(\lambda_{\theta,\text{ max}} - \lambda_\theta)^{-1}}$$

was proposed, where $\lambda_{\theta,\text{ max}}$, c_{inel}, and $\lambda_{\text{el, max}}$ are the model constants; λ_θ and λ_z are the elongations in the circumferential and axial directions, respectively.

In [21], the vein wall was represented by a set of elastic fibers oriented along the vessel axis and connected between themselves by rigid inextensible elements. The idea of representing soft tissues by a set of elastic fibers was earlier used for modeling heart tissues (see [22, 23]). Such a representation of the vessel wall was used for solving the problem of the influence of the cava filter on blood flow (see [24]) and in the study of hemodynamics in the network of arterial vessels with atherosclerotic plaques (see [25]).

Among the works devoted to the constitutive equations for veins, we note [16, 26–28]. The majority of the proposed constitutive equations for veins are based on the arterial models described above. However, another phenomenological model was proposed in [27] based on the experimental data obtained for the sheep suprarenal vein:

$$\Psi = \mu(I_1 - 3) + D_2(\sqrt{I_4} - 1)^2 + D_3(\sqrt{I_6} - 1)^2.$$

Let us briefly discuss the modeling of passive–active properties of blood vessel walls; these properties are due to smooth muscular cell contractions. This contraction is a response to various chemical stimuli, and it contributes to the stress in the vessel walls (see Fig. 5). This contraction results in a considerable reduction of the stress gradient in the vessel walls (see [11, 14]). The same effect is obtained when the residual stresses in the vessel walls are taken into account (see [11]).

In distinction from passive properties, the constitutive equations for the passive–active properties of blood vessels are given less attention. The description of currently available equations can be found in [29]. It is assumed that the elastic deformation energy is an additive quantity:

$$\Psi = \Psi_{\text{passive}} + \Psi_{\text{active}},$$

Table 1. Generalized dependence of the pressure and squared pulse wave propagation rate on the cross section for arteries: *1* was used in [1, 2, 37] and others; *2* in [30]; *3* in [31, 33, 34, 38–40] and others; *4* in [32, 35, 36] and others. The constant α was determined by matching the data in [41] (see curve *5* in Fig. 6)

No.	$P(\eta)$	$c^2(\eta)$	α, kPa (CCA)	α, kPa (CFA)
1	$\alpha(\eta - 1)$	$\alpha\eta$	25.8080	33.3330
2	$\alpha\left(1 - \frac{1}{\sqrt{\eta}}\right)$	$\frac{\alpha}{2\sqrt{\eta}}$	70.3217	64.5750
3	$\alpha(\sqrt{\eta} - 1)$	$\frac{\alpha\sqrt{\eta}}{2}$	57.4200	72.7695
4	$\alpha(\exp(\eta - 1) - 1)$	$\alpha\eta\exp(\eta - 1)$	19.8916	25.1076

Table 2. Generalized dependence of the pressure and squared pulse wave propagation rate on the cross section of the canine femoral vein: *1* was used in [37]; *2* in [45]; *3* in [46]; *4* in [32, 35, 36] and others. The values of the coefficients for model [45] were found using the least squares method and data [43, 44]. The constant α was determined by matching the data in [43, 44] (see curve *5* in Fig. 8a)

No.	$P(\eta)$	$c^2(\eta)$	α, kPa (OCA)
1	$\alpha\left(1 - \frac{1}{\eta^{3/2}}\right)$	$\frac{3\alpha}{2\eta^{3/2}}$	7.210
2	$a\eta^3 + b\eta^2 + c\eta$	$3a\eta^3 + 2b\eta^2 + c\eta$	−22.091 (kPa), 53.022 (kPa), −31.170 (kPa)
3	$\alpha\left(\eta^{10} - \frac{1}{\eta^{3/2}}\right)$	$\alpha\left(10\eta^{10} + \frac{3}{2\eta^{3/2}}\right)$	1.501
4	$\alpha\ln\eta$	α	11.7169

Here, Ψ_{passive} describes the passive properties (using, e.g., the model proposed in [9]), and Ψ_{active} describes the contribution of smooth muscular cells. A possible representation of Ψ_{active} is

$$\Psi_{\text{active}} = S([A])f(\lambda_f),$$

where $S([A])$ is the activation function due to the concentration of the vasoconstrictor element $[A]$ and $f(\lambda_f)$ is a cubic polynomial of the elongation of smooth muscular cells λ_f.

Based on the above discussion, we conclude that all the constitutive equations (both for passive and passive–active walls) describe the increase in the rigidity of vessels due to the involvement of collagen fibers when the transmural pressure increases. In this case, the slope of the tangent to the deformation curve increases (e.g., see Fig. 5). At the physiological level of pressure, both the elastin and collagen are involved in the load distribution in the artery wall. The available constitutive equations are based on the experimental data for the tissue deformation, and they are phenomenological. The constitutive equations are constructed with regard to the microstructure of vessel walls. The development of this approach is complicated by the requirement to have data of immunohistochemical examination, which are impossible to obtain for individual patents. For venous constitutive equations, arterial models are mainly used; however, it is not always valid because of different anatomic structure and functional properties of arteries and veins.

4. VESSEL ELASTICITY IN ONE-DIMENSIONAL MODELS OF HEMODYNAMICS

During the last decades, a number of one-dimensional models for the blood flow in the vascular bed have been developed (see [1, 30–34] and others). Under this approach, the blood flow is considered as the flow of incompressible fluid in the network of elastic tubes. The models are constructed on the basis of mass and momentum conservation laws in an isolated vessel and are then extended for the network by stat-

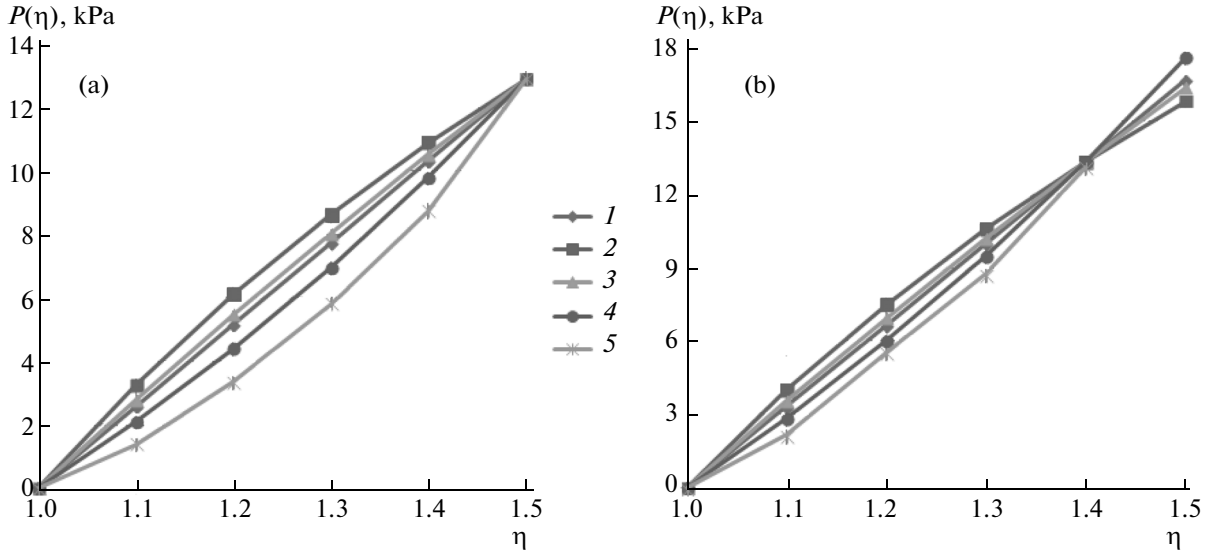

Fig. 6. Pressure in the common carotid artery (a) and common femoral artery (b). Curves 1–4 correspond to the rows in Table 1; 5 corresponds to the data in [41].

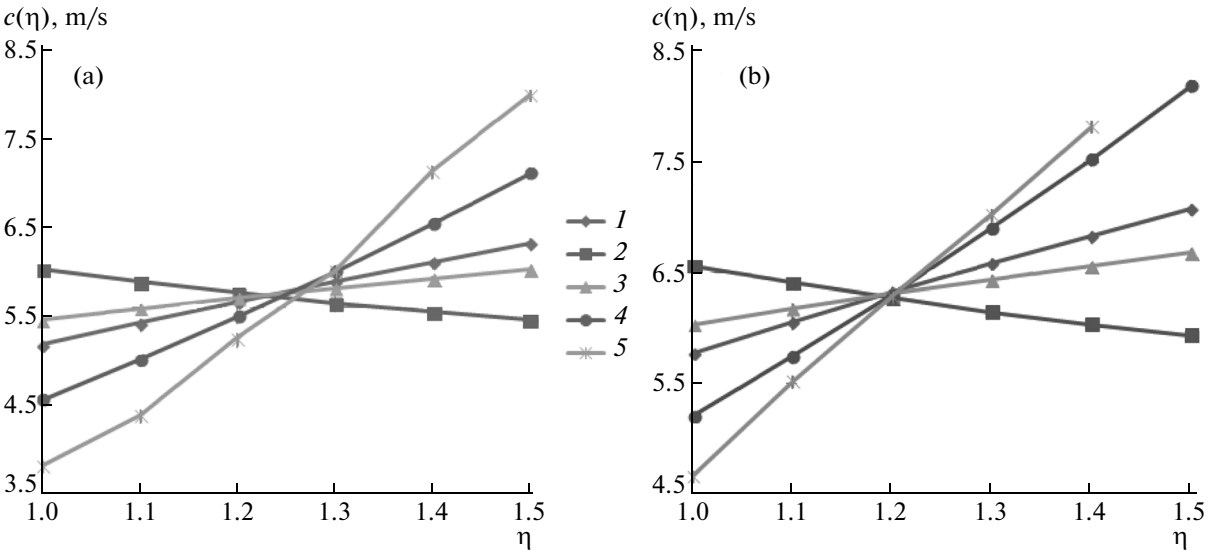

Fig. 7. Pulse wave propagation rate for the common carotid artery (a) and common femoral artery (b). Curves 1–4 correspond to the rows in Table 1; 5 was calculated approximately with the second order of accuracy based on the data in [41].

ing boundary conditions at the junctions of the vessel with other vessels, with the heart and microcirculation regions. Here is a possible mathematical statement:

$$\partial S/\partial t + \partial(Su)/\partial x = f_s, \tag{4.1}$$

$$\partial u/\partial t + \partial(u^2/2 + P(S)/\rho)/\partial x = f_u, \tag{4.2}$$

Here, t is the time, x is the coordinate along the vessel, $\rho \approx 1$ g/cm^3 is the blood density, $S(t, x)$ is the vessel cross section, $u(t, x)$ is the linear blood flow velocity averaged over the cross section under the assumption of the Poiseuille profile, P is the pressure, f_s is the source or sink of mass per the unit vessel length, and f_u is the flow acceleration due to various forces. In this paper, we assume that $f_s = 0$ and $f_u = 0$.

In the construction of such models, an important phase is to close the hyperbolic system (4.1), (4.2) by introducing a function $P(S)$ determining the pressure in a vessel cross section depending on the area of

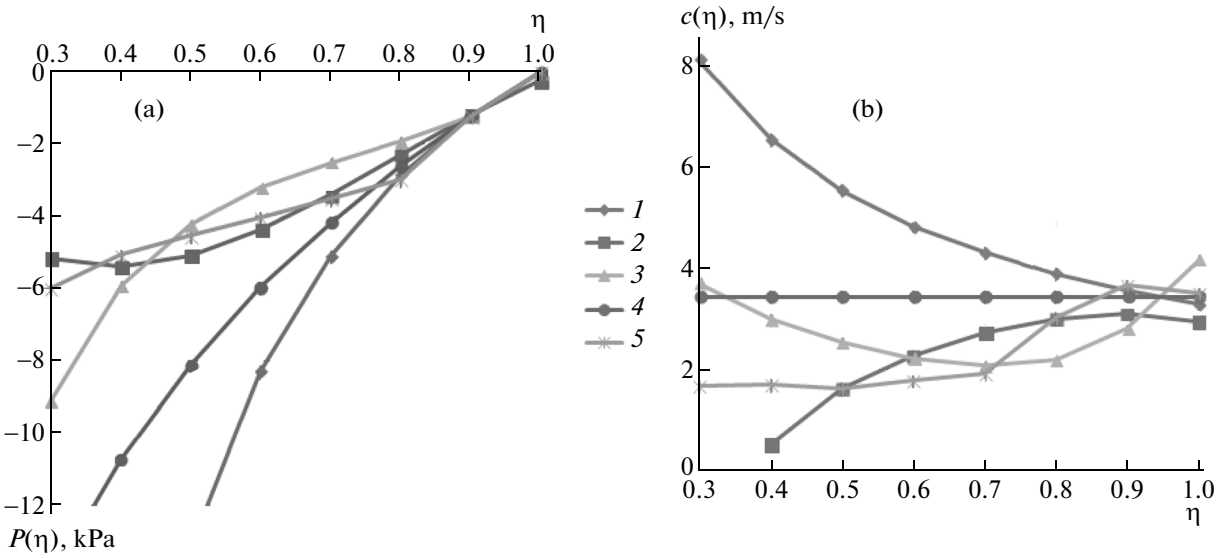

Fig. 8. Pressure $P(\eta)$ (a) and pulse wave propagation rate (b) in the canine femoral vein. Curves 1–4 correspond to rows in Table 2, and 5 corresponds to the data in [43, 44].

this cross section. The form of $P(S)$ is determined by the elastic properties of the vessel wall. This function can be obtained for each specific vessel using the approaches described in Section 3; however, this requires data about the structure of the vessel wall. The function $P(S)$ can be determined more accurately by direct simultaneous measurements of P and S. However, due to limitation of the modern diagnostics means, the use of such approaches for the construction of an individual model of a specific patent, which should include at least several tens of large arteries and veins, is difficult. In the majority of studies, $P(S)$ is obtained empirically or by simplifying the combined elastic models described in Section 3. In most cases, $P(S)$ can be written as

$$P(S) = P_0 + f(\alpha, \eta(S)), \tag{4.3}$$

where $P_0 = \text{const}$, $\alpha = \text{const}$, and $\eta(S) = S/S_0$.

The values for P_0, α, and S_0 should be specified for each vessel, depending on its anatomic features and elastic properties. Tables 1 and 2 present the most widespread expressions for $f(\alpha, \eta)$ upon reducing $P(S)$ used in different works to form (4.3). The values for P_0, α, and S_0 are determined using the data of medical examinations for the human common carotid artery (CCA), human common femoral artery (CFA) (see [41, 42]), and the canine common femoral vein (see [43, 44]). For the arteries with circular cross section, it was assumed that $\eta \geq 1$; and for the veins with an elliptic cross section, $\eta < 1$ (see [37]).

For the CCA, $S_0 = 0.2165$ cm^2 was used, for the CFA we used $S_0 = 0.3578$ cm^2, and for the vein common femoral artery $S_0 = 0.229$ mm^2. In all the cases, $P_0 = 6.666118$ kPa. The values of all the constants, including the values of α shown in Tables 1 and 2, were chosen so as to make the curves $P(S)$ to pass through the same values of the minimum and maximum pressures obtained experimentally [41–44]. The form of functions $P(S)$ obtained for these values of parameters for the CCA and CFA is illustrated in Fig. 6; for the canine common femoral vein, it is shown in Fig. 8a. The indexes of curves in Figs. 6 and 8a correspond to the rows in Tables 1 and 2, respectively.

An important factor for the analysis of the influence of the form of $P(S)$ on the wave pattern in the case of pulsating flow of viscous incompressible fluid in the network of elastic tubes is the propagation rate of the pulse wave (the propagation rate of small perturbations in the vessel wall) in each tube of the network. This parameter can be found by calculating eigenvalues of the Jacobian matrix of system (4.1), (4.2) (for details see, e.g., [1, 34, 36, 39]):

$$c(\eta) = \sqrt{\frac{\eta}{\rho}\frac{\partial P}{\partial \eta}}.$$

It is seen from Figs. 6 and 8a that the curves corresponding to different functions $P(S)$ differ only insignificantly. By using various criteria for the choice of model constants, one can make the curves almost identical at $\eta \approx 1$. The difference becomes significant in the analysis of $c(\eta)$ for different cases. In Figs. 7

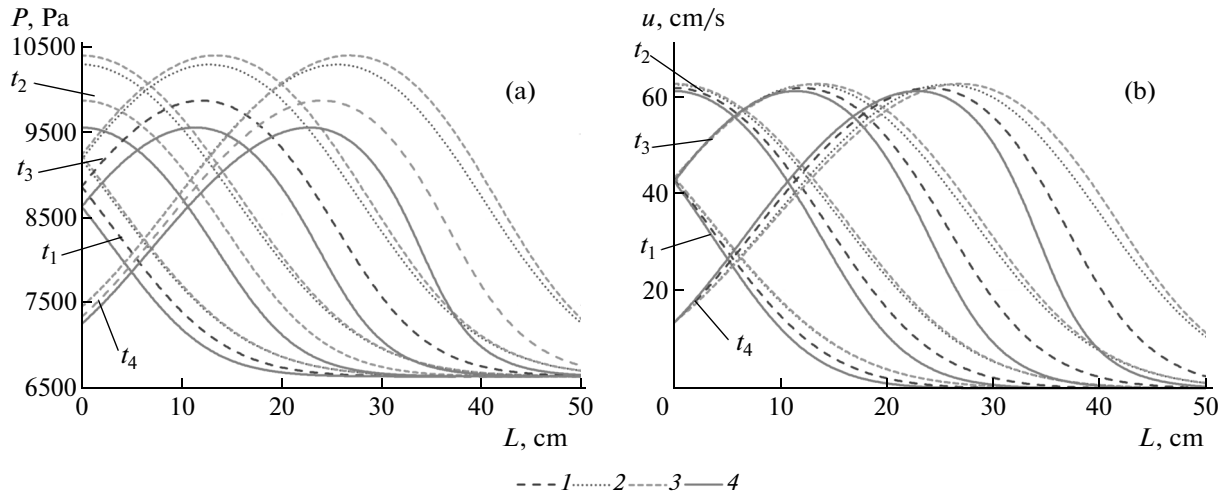

Fig. 9. Pressure and rate in the common carotid artery for various state equations. $t_1 = 0.8$ s, $t_2 = 1.0$ s, $t_3 = 1.2$ s, $t_4 = 1.4$ s. 1 corresponds to [1, 2, 37] and others, 2 to [30],; 3 to [38,31, 39, 40, 33, 34] and others, 4 to [35, 32, 36] and others.

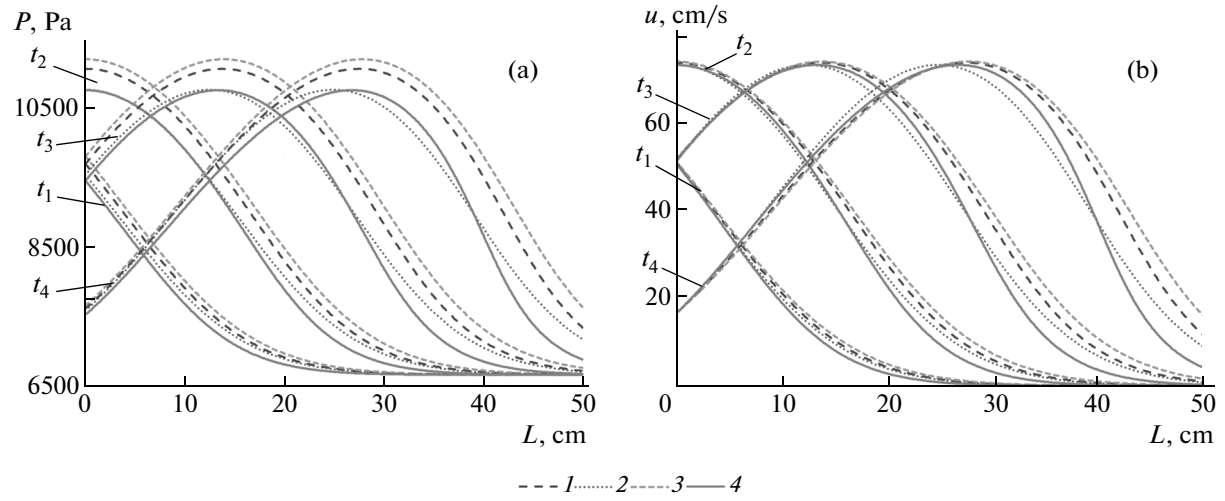

Fig. 10. Pressure and rate in the common femoral artery for various state equations. $t_1 = 0.8$ s, $t_2 = 1.0$ s, $t_3 = 1.2$ s, $t_4 = 1.4$ s. 1 corresponds to [37], 2 to [45], 3 to [46], 4 to [32, 35, 36] and others.

and 8b one can see significant differences of the dependences of the pulse wave propagation on the cross section. These differences persist even for the constants at which $P(S)$ are almost identical at $\eta \approx 1$. Thus, calculations based on different models of wall elasticity can yield significantly different results.

To test various models, the numerical discretization of system (4.1), (4.2) using the grid-characteristic method of the second approximation order (see [47]) was used. A fairly long elastic tube ($L = 100$ cm) was considered. At its left endpoint, the flow was specified by

$$Q_{\text{in}}(t) = Q_0 \exp(-10^3 (t - 0.1)^2), \quad t \geq 0, \tag{4.4}$$

where $Q_0 = 15$ mL/s was used for the common carotid artery and $Q_0 = 30$ mL/s for the common femoral artery; this agrees with typical conditions in the cardiovascular system in humans. Along with condition (4.4), an explicit second-order approximation of the consistency condition for the hyperbolic system (4.1), (4.2) (see [32, 36]) along the characteristic leaving the domain was set at the left endpoint of the tube. The boundary conditions at the right endpoint of the tube can be set arbitrarily in our case. The tube length was chosen such that the boundary conditions at the right endpoint do not affect the solution near the left endpoint (in the range from 0 through 40 cm) during the observation period.

The numerical results are illustrated in Figs. 9 and 10. Wave patterns at the times $t_1 = 0.8$ s, $t_2 = 1.0$ s, $t_3 = 1.2$ s, and $t_4 = 1.4$ s from the time when pulse (4.4) begins. The differences are more clearly seen in the simulation of the propagation of a solitary pulse in the common carotid artery (Fig. 9). Differences both in the pressure amplitude and in the pulse wave propagation rate are seen. Note that the leading edge (right-hand part) of the wave front is significantly steeper in case 4.

According to elasticity model 4 (see Table 1), the pulse wave propagation rate is higher in the domain when the cross section is stretched, which results in the wave running on the leading edge with the subsequent formation of the shock wave. The same effect is observed in the other cases because qualitatively the function $P(S)$ for vessels is monotone (see [37]). However, the shock wave is generated much farther (several meters), which is beyond the physiological range. Nevertheless, it is known that in some pathological cases related to the increased rigidity of arterial walls, increase of the left ventricle stroke volume, in the case of stenotic vessel involvement, and other cases, a shock wave can occur within several tens of centimeters from the heart. For the numerical simulation of such cases within the one-dimensional hemodynamic models, the elasticity model $P(S)$ must be analyzed more thoroughly.

In the case of the common femoral artery (Fig. 10), the pattern is somewhat different. The spread of the curves corresponding to different cases is less significant. The differences in the pressure levels and in the pulse wave propagation rates are also less significant. The trend to the formation of a shock wave is again most well defined for model 4 (see Table 1). It seems that this is due to the greater cross section of the common femoral artery compared with the common carotid artery. The differences become visible far beyond the physiologically feasible range.

5. CONCLUSIONS

Computational experiments described in this paper for the common carotid and femoral arteries suggest that various elasticity models represented by functions $P(S)$ yield satisfactory results in the physiologically admissible range of parameters conditionally corresponding to normal conditions. The differences between models become detectable in the cases of pathological changes in heart functions, elastic properties of vessel walls, and stenotic vessel involvement. In the simulation of such cases, the validity of the elasticity model should be verified using medical examinations, and the underlying mathematical model should be more complex and match the physical models of vessel wall elasticity described in Section 3.

However, a number of factors reduce the need for more accurate simulation of elasticity in one-dimensional models than was described in Section 4. The propagation of pulse waves and blood flow in the modes that are close to the formation of shock waves are considerably affected by such factors as blood viscosity, visco-elasticity of vessel walls, longitudinal extensibility of vessels, and autoregulation, which are beyond the scope of this paper.

The simulation of venous blood flow by analogy with arterial flow in this paper is difficult because some of the vein elasticity models do not cover the case $\eta > 1$ (circular cross section). In the case of veins, the proposed comparison technique based on the calculation of solitary pulse propagation is inadequate because there are almost no wave flows in veins. On the other hand, the venous blood flow is significantly affected by such factors as venous valves, the sucking effect of the heart, and the muscle pump effect, which require the development of new experiments.

ACKNOWLEDGMENTS

This work was supported by the Russian Science Foundation, project no. 14-31-00024. The numerical simulation in Section 4 was supported by the Russian Foundation for Basic Research, project nos. 14-01-00830, 14-11-00877, 14-01-00779).

REFERENCES

1. M. V. Abakumov, K. V. Gavrilyuk, N. B. Esikova, V. B. Koshelev, A. V. Lukshin, S. I. Mukhin, N. V. Sosnin, V. F. Tishkin, and A. P. Favorskii, "Mathematical models of hemodynamics of the cardiovascular system," Differ. Uravn. **7** (33), 892–898 (1997).
2. I. V. Ashmetkov, N. B. Esikova, V. F. Tishkin, M. V. Abakumov, I. V. Ashmetkov, N. V. Esikova, V. V. Koshelev, S. I. Mukhin, N. V. Sosnin, V. F. Tishkin, A. P. Favorskii, and A. B. Khrulenko, "A strategy for modeling the cardiovascular system," Mat. Modelir. **12** (2), 106–117 (2000).
3. I. V. Ashmetkov, A. Ya. Bunicheva, V. A. Lukshin, V. V. Koshelev, S. I. Mukhin, N. V. Sosnin, A. P. Favorskii, and A. B. Khrulenko, *Mathematical modeling of blood circulation using the CVSS software package,"* in *Computer Models and Advances in Medcine* (Nauka, Moscow, 2001), pp. 194–218 [in Russian].

4. I. V. Ashmetkov, S. I. Mukhin, N. V. Sosnin, and A. P. Favorskii, "A boundary value problem for the linearized haemodynamic equations on a graph," Differ. Equations **40** (1), 94–104 (2004).
5. A. Ya. Bunicheva, M. A. Menyailova, S. I. Mukhin, N. V. Sosnin, and A. P. Favorskii, "Studying the influence of gravitational overloads on the parameters of blood flow in vessels of greater circulation," Math. Models Comput. Simul. **5**, 81–91 (2013).
6. Blausen.com staff, "Blausen gallery 2014", Wikiversity Journal of Medicine. DOI:10.15347/wjm/2014.010
7. J. A. G. Rhodin, "Architecture of the vessel wall," in *The Handbook of Physiology. The Cardiovascular System* (Bethesda, Maryland, 1980), Vol. 2, pp. 1–31.
8. R. P. Vito and S. A. Dixon, "Blood vessel constitutive models—1995-2002," Ann. Rev. Biomedical Eng. **5** (1), 413–439 (2003).
9. G. A. Holzapfel, "Biomechanics of soft tissue," in *The Handbook of Materials Behavior Models*, (2001), Vol. 3, pp. 1049–1063.
10. M. R. Roach, "The reason for the shape of the distensibility curves of arteries," Can. J. Biochemistry Physiol. **35**, 681–690 (1957).
11. J. D. Humphrey, "Review paper: Continuum biomechanics of soft biological tissues," Proc. R. Soc. London, Ser. A **459** (2029), 3–46 (2003).
12. G. A. Holzapfel and R. W. Ogden, "Constitutive modelling of arteries," Proc. R. Soc. London, Ser. A **466** (2118), 1551–1597 (2010).
13. P. Kalita and R. Schaefer, "Mechanical models of artery walls," Arch. Comput. Meth. Eng. **15** (1), 1–36 (2008).
14. H. Chen, X. Zhao, X. Lu, Y. Huo, and G. S. Kassab, "Microstructural constitutive model of active coronary media," Biomaterials **34** (31), 7575–7583 (2013).
15. Y. Hollander, D. Durban, X. Lu, G. S. Kassab, and Y. Lanir, "Constitutive modeling of coronary arterial media-comparison of three model classes," J. Biomech. Eng. **133** (6), 061008 (2011).
16. D. P. Sokolis, "Experimental investigation and constitutive modeling of the 3d histomechanical properties of vein tissue," Biomech. Model. Mechanobiology **12** (3), 431–451 (2013).
17. C. J. Ghuong and Y. C. Fung, "Three-dimensional stress distribution in arteries," J. Biomech. Eng. **105** (3), 268–274 (1983).
18. G. A. Holzapfel, T. C. Gasser, and R. W. Ogden, "A new constitutive framework for arterial wall mechanics and a comparative study of material models," J. Elasticity Phys. Sci. Solids **61** (1-3), 1–48 (2000).
19. T. G. Gasser, R. W. Ogden, and G. A. Holzapfel, "Hyperelastic modelling of arterial layers with distributed collagen fibre orientations," J. R. Soc. Interface **3** (6), 15–35 (2006).
20. G. A. Holzapfel, G. Sommer, and P. Regitnig, "Determination of layer-specific mechanical properties of human coronary arteries with nonatherosclerotic intimal thickening and related constitutive modeling," Am. J. Physiol., Ser. Heart and Circulatory Physiol. **289**, H2048–H2058 (2005).
21. G. W. Desch and H. W. Weizsacker, "A model for passive elastic properties of rat vena cava," J. Biomech. **40** (14), 3130–3145 (2007).
22. D. M. McQueen, "A three-dimensional computational method for blood flow in the heart i. immersed elastic fibers in a viscous incompressible fluid," J. Comput. Phys. **81** (2), 372–405 (1989).
23. D. M. McQueen and C. S. Peskin, "A three-dimensional computational method for blood flow in the heart. II. Contractile fibers," J. Comput. Phys. **82** (2), 289–297 (1989).
24. Y. V. Vassilevski, S. S. Simakov, and S. A. Kapranov, "A multi-model approach to intravenous filter optimization," Int. J. Numer. Meth. Biomedical Eng. **26** (7), 915–925 (2010).
25. Y. Vassilevski, S. Simakov, V. Salamatova, Y. Ivanov, and T. Dobroserdova, "Vessel wall models for simulation of atherosclerotic vascular networks," Math. Modell. Natural Phenomena **6** (7), 82–99 (2011).
26. A. Agianniotis, R. Rezakhaniha, and N. Stergiopulos, "A structural constitutive model considering angular dispersion and waviness of collagen fibres of rabbit facial veins," Biomedical Eng. Online **10** (1), 18 (2011).
27. V. Alastrué, E. Peña, M. A. Martínez, and M. Doblaré, "Experimental study and constitutive modelling of the passive mechanical properties of the ovine infrarenal vena cava tissue," J. Biomech. **41** (14), 3038–3045 (2008).
28. K. McGilvray, R. Sarkar, K. Nguyen, and C. M. Puttltz, "A biomechanical analysis of venous tissue in its normal and post-phlebitic conditions," J. Biomech. **43** (15), 2941–2947 (2010).
29. Z. Yosibash and E. Priel, "Artery active mechanical response: high order finite element implementation and investigation," Comput. Meth. Appl. Mech. Eng. **237**, 51–66 (2012).
30. M. S. Olufsen, C. S. Peskin, W. Y. Kim, E. M. Pedersen, A. Nadim, and J. Larsen, "Numerical simulation and experimental validation of blood flow in arteries with structured-tree outflow conditions," Annal. Biomedical Eng. **28**, 1281–1299 (2000).
31. L. Formaggia, A. Quarteroni, and A. Veneziani, *Cardiovascular Mathematics* (Springer, Heidelberg, 2009), Vol. 1.

32. A. S. Kholodov, "Dynamical models of external respiration and blood circulation taking into account their interrelations and transport of substances," in *Computer Models and Advances in Medicine* (Nauka, Moscow, 2001), pp. 127–163 [in Russian].
33. J. Alastruey, K. H. Parker, J. Peiró, and S. J. Sherwin, "Lumped parameter outflow models for 1-D blood flow simulations: Effect on pulse waves and parameter estimation," Commun. Comput. Phys. **4** (2), 317–336 (2008).
34. L. O. Müller, "Well-balanced high-order numerical schemes for one-dimensional blood flow in vessels with varying mechanical properties," J. Comput. Phys. **242**, 53–85 (2013).
35. S. S. Simakov, A. S. Kholodov, and A. V. Evdokimov, "Techniques for the calculation of global blood flow in humans using heterogeneous computational models," in *Medicine in the Mirror of Information Science* (Nauka, Moscow, 2008), pp. 124–170 [in Russian].
36. S. S. Simakov and A. S. Kholodov, "Computational study of oxygen concentration in human blood under low frequency disturbances," Math. Models Comput. Simul. **1**, 283–295 (2009).
37. T. J. Pedley and X. Y. Luo, "Modelling flow and oscillations in collapsible tubes," Theor. Comput. Fluid Dynamics **10**, 277–294 (1998).
38. L. Formaggia, D. Lamponi, and A. Quarteroni, "One-dimensional models for blood flow in arteries," J. Eng. Math. **47**, 251–276 (2003).
39. J. P. Mynard and P. Nithiarasu, "A 1D arterial blood flow model incorporating ventricular pressure, aortic valve and regional coronary flow using the locally conservative Galerkin (LCG) method," Commun. Numer. Meth. Eng. **24** (5), 367–417 (2008).
40. I. Larrabidea, P. J. Blanco, and S. A. Urquiza, E. A. Dari, M. J. Véneref, N. A. de Souza e Silvac, and R. A. Feijóo, "HeMoLab—hemodynamics modelling laboratory: An application for modelling the human cardiovascular system," Comput. Biology Medicine **42**, 993–1004 (2012).
41. R. Armentano, J. L. Megnien, A. Simon, F. Bellenfant, J. Barra, and J. Levenson, "Effect of hypertension on viscoelasticity of carotid and femoral arteries in humans," Hypertension **26**, 48–54 (1995).
42. P. Studinger, Z. Lénárd, Z. Kováts, L. Kocsis, and M. Kollai, "Static and dynamic changes in carotid artery diameter in humans during and after strenuous exercise," J. Physiol. **550**, 575–583 (2003).
43. P. Dobrin, F. N. Littooy, J. Golan, and J. Fareed, "Mechanical and histologic changes in canine vein grafts," J. Surgical Res. **44** (3), 259–265 (1988).
44. P. Dobrin, "Mechanics of Normal and Diseased Blood Vessels," Annal. Vascular Surgery **2** (3), 283–294 (1988).
45. J. Fernandez, P. Hunter, V. Shim, and K. Mithraratne, "A subject-specific framework to inform musculoskeletal modeling: outcomes from the IUPS physiome project," in *Patient-Specific Computational Modeling*, Ed. by C. Lopes, and Â. Pena (Springer, Netherlands, 2012).
46. L. O. Muller, "A global multiscale mathematical model for the human circulation with emphasis on the venous system," Int. J. Numeric. Meth. Biomedical Eng. **30** (7), 681–725 (2014).
47. K. M. Magomedov and A. S. Kholodov, *Grid-Characteristic Numerical Methods* (Nauka, Moscow, 1988) [in Russian].

Translated by A. Klimontovich